

SURFACE AND SUBSURFACE ALTERATIONS INDUCED BY HARD TURNING OF AISI 52100 BEARING STEEL

SAULO P. TRINDADE¹, KLAUS H.S. SILVA^{1,2}, DIOGO A. OLIVEIRA^{1,2},
ALEXANDRE M. ABRÃO^{1,*}

¹Department of Mechanical Engineering, Universidade Federal de Minas Gerais, Av.
Antônio Carlos, 6627, Pampulha, Belo Horizonte MG, CEP: 31270-901, Brazil

²Department of Mechanical Engineering, Pontifical Catholic University of Minas Gerais, Rua
Dom José Gaspar, 500, Coração Eucarístico, Belo Horizonte, MG, CEP 30535-901, Brazil

*Corresponding Author: abrao@ufmg.br

Abstract

Over the last decades, turning of hardened steel for finishing purposes has earned visibility as a process that can potentially match grinding. This is due to the fact that economic advantages can be obtained when turning instead of grinding, however, turning of hardened steels has not been able to replace grinding to a greater extent owing to the difficulty of the former in providing the same level of dimensional accuracy achieved by the latter. The aim of this work is to assess the influence of cutting parameters (cutting speed, feed and depth of cut) on the dimensional and geometric deviations induced by finish turning of hardened AISI 52100 steel (60 HRC) with mixed alumina ($Al_2O_3 + TiC$) cutting tools. Additionally, the influence of the cutting parameters on the microstructure and subsurface microhardness profile is investigated. The novelty of the present work is to establish a relationship between surface (dimensional and geometric deviations) and subsurface (microstructure and microhardness variation) alterations induced by hard turning, which are crucial to the performance of the machined component. The results show that feed significantly affects diameter deviation, circularity, concentricity and surface roughness, while depth of cut affects diameter deviation and parallelism error. The influence of cutting speed is significant only with regard to the concentricity error. As far as subsurface alterations are concerned, higher surface microhardness values were obtained when combining higher cutting speed and lower feed and depth of cut. Clear evidence of microstructure alterations was observed under the most severe cutting condition only.

Keywords: Dimensional and geometric deviations, Hardened steel, Microhardness, Microstructure, Turning.

1. Introduction

Given the ever-increasing demand for lower production costs, attention has been given to turning as an alternative to grinding of hardened steels for finishing purposes. Turning allows higher material removal rates than grinding, reducing cycle times and leading to increased productivity and costs reduction, which brings economic benefits. Conversely, the infinitesimal undeformed chip thickness achieved by grinding during the sparking out cycle leads to the production of components with superior dimensional and geometric quality.

Finish turning of hardened steel is applied to materials which hardness ranges from 45 to 68 HRC [1] and has only become possible after the development of polycrystalline cubic boron nitride (PcBN) tools, since conventional tungsten carbide tools are subjected to accelerated wear rates due to high temperatures at tool-chip interface and strong adhesion of the chip on the rake face [2]. Polycrystalline cubic boron nitride and alumina based ceramics tools, such as titanium carbide reinforced aluminum oxide ($\text{Al}_2\text{O}_3 + \text{TiC}$), possess high hot hardness, wear resistance and chemical stability at high temperatures, features required to tackle hardened steels.

The principal characteristics of finish turning of hardened steels are high cutting speed, low feed and low depth of cut and its main advantages are related to high material removal rate, high quality of the machined surface, ability to produce complex geometries without the use of special tools, short set-up time, possibility to perform both finishing and ordinary operations with a single set-up, absence of cutting fluid, reduced production costs and high productivity. Total processing time for hard turning can be as little as 60% of grinding for the same part [3-5]. On the other hand, hard turning poses the following drawbacks: high temperatures are generated at the cutting edge and elevated cutting forces arise in the process due to the high hardness of the work material. Moreover, elevated cutting speeds lead to even higher temperatures at the tool-chip interface. These two aspects promote accelerated wear rates, formation of white layer and larger dimensional and geometric errors in comparison with grinding. White layer is a thin layer generated on the workpiece surface, which presents higher hardness than that of the material underneath, being formed by a phase transformation rich in retained austenite (γ -phase iron) due to the elevated temperatures [1]. On components that must endure high contact stress, white layer delamination might occur, causing component failure. According to Guo et al. [6], parts with white layer could have a fatigue life eight times shorter in comparison with those without it.

Generally speaking, dimensional and geometric errors are introduced due to inappropriate selection of cutting parameters, elevated cutting forces, low machine and fixture stiffness, thermal expansion of the part and severe cutting tool wear. The relationship between error sources and causes is complex and difficult to track because the effects are interconnected. Zhou et al. [3] suggest the following line of thought to understand these relationships: worn tools cause dimensional errors due to a change in the effective depth of cut and also promote the elevation of cutting forces and temperatures by increasing tool/workpiece contact surface; while cutting forces increase leads to dimensional errors due to elevated elastic deformation of the workpiece and machine tool; finally, temperature increase causes errors by thermal expansion of the workpiece and speeds up tool wear.

Tool wear causes the loss of the effective depth of cut, which leads to dimensional and geometric errors due to a shift in alignment between the tool tip and the part [3]. Moreover, tool wear causes an increase of both cutting forces and temperature, two factors that independently cause dimensional and geometric errors. When tool wear worsen, so does dimensional errors.

Bernardos et al. [7] describe the variation in depth of cut induced by cutting force: under the influence of the passive force, the workpiece starts to deform elastically the instant the tool tip touches it. The passive force pushes the workpiece away from the tool tip, thus reducing the effective depth of cut. When rough turning, reduced depth of cut causes a decrease in cutting forces, including the passive force, which in turn causes a decrease in the part's elastic deformation leading to an increase of the effective depth of cut. Consequently, cutting forces increase again and the depth of cut variation effect occurs in a cycle. The result is an oversized component with accentuated circularity deviation.

High cutting forces also present a challenge when the machine tool stiffness does not meet the process requirements and can lead to accelerated degradation of the machine movable parts. Fan et al. [8] correlate turning forces with the deformations of the machine tool bed ways, which leads to errors in tool path and, finally, to dimensional and geometric errors on the final part. According to Kalyan Kumar and Choudhury [9], the increase in cutting speed causes a reduction of the coefficient of friction between workpiece and cutting tool, thus increasing the shear angle, reducing the shear area and, consequently, turning force components. Henzold [10] reported a reduction of circularity deviation when cutting speed was elevated. On the other hand, elevated feed and depth of cut values lead to an increase in material removal rate also causing an increase in the plastic deformation rate and resulting in higher cutting forces. Therefore, lower dimensional deviations are expected to be obtained by reducing cutting forces.

According to Weck et al. [11], the contribution of thermal effects on total errors of the final part can reach 50%. High cutting temperatures might cause an undesirable expansion of the machined part and tool, increasing effective depth of cut and dimensional variation of the finished component. This effect is boosted by the absence of cutting fluid. Zhou et al. [3] report that tool and part temperature can be reduced by 70% simply by using cutting fluid during the process, thus promoting a reduction in dimensional errors by 50% when compared to dry cutting.

High cutting temperatures are caused mainly by two factors: tool wear and high cutting speeds. Using a two-color pyrometer to measure cutting edge temperature while turning AISI 52100 steel, Ueda et al. [12] noticed that increasing cutting speed from 100 m/min to 300 m/min caused the cutting edge temperature to increase from 800 °C to 950 °C. Similar results were found by Müller et al. [13] when turning AISI 1045 steel and by Han et al. [14] working on AISI 1045, albeit using thermocouples to conduct temperature measurements.

Hosseini et al. [4] investigated the influence of cutting speed and tool wear on cutting temperature when turning AISI 52100 steel using fresh and worn cutting tools. The results show a steep rise in temperature when cutting speed was increased from 30 m/min to 110 m/min (with higher temperature values recorded for worn tools) than when increasing cutting speed from 110 m/min to 260 m/min (in this case the difference between fresh and worn tools was not statistically significant). Moreover,

a temperature rise of approximately 300 °C using fresh tools and of 400 °C using worn tools was noted when cutting speed increased from 30 m/min to 260 m/min.

In addition to dimensional and geometric errors, the combination of high turning forces and temperature may cause alterations in the layer beneath the surface. In the case of forces, severe plastic deformation may promote work hardening, whereas high temperatures followed by rapid cooling may produce untempered martensite if the austenization temperature is reached and the carbon content is sufficiently high. Umbrello and Filice [15] report that the thickness of the untempered martensite layer increases with cutting speed and feed in dry orthogonal cutting of hardened ASI 52100 steel with PcBN compacts, nevertheless, Biček et al. [16] state that untempered martensite is not present when turning the same material under cryogenic environment.

The main goal of this work is to assess the influence of cutting speed, feed and depth of cut on dimensional (diameter) and geometric deviations (circularity, parallelism, concentricity and roughness) attained after finish turning quenched and tempered AISI 52100 bearing steel (average hardness of 60 HRC) using mixed alumina cutting tools ($\text{Al}_2\text{O}_3 + \text{TiC}$). Moreover, the influence of the cutting parameters on the workpiece microstructure and subsurface microhardness profile is investigated. As a result it will be possible to assess how close turning can get of grinding (with regard to dimensional and geometric deviations) when machining hardened bearing steel and to identify the cutting parameters responsible for attaining, simultaneously, best surface quality and minimum damage induced beneath it.

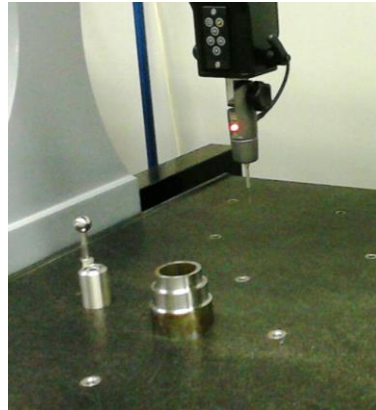
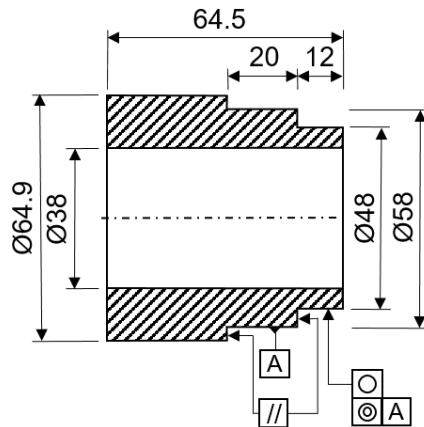
2. Experimental Procedure

Twenty tubular blanks of AISI 52100 bearing steel with 64.9 mm external diameter, 38 mm internal diameter and 65 mm long were used as work material. The blanks were initially subjected to quenching and tempering in order to achieve an average hardness of 60 ± 2 HRC. Prior to the tests, rough turning was carried out in order to produce samples with an oversize corresponding to the depth cut to be employed in the conclusive tests. Finish turning tests were performed on a computer numerical control lathe (5.5 kW power and 3500 maximum rotational speed) using titanium carbide reinforced aluminum oxide ceramic tools (Sandvik Coromant grade CC650) with geometry code TNGN 16 04 08T01020 (chamfer of $0.10 \text{ mm} \times 20^\circ$). Cutting speed, feed and depth of cut were the factors investigated using a 2^3 factorial design of experiments with two replicates plus four central runs. Table 1 indicates the chosen cutting parameters, selected based on the cutting tool manufacturer recommendations [17]. Montgomery [18] reports that 2^k factorial designs are especially useful in the early stages of experimental work, when there are likely to be many factors to be investigated. It provides the smallest number of runs, however, the response is assumed approximately linear. On the other hand, 3^k factorial designs should be used when there is concern about curvature in the response function, however, this design is not the most efficient way to model a quadratic relationship (this can be obtained with a 2^k design with augmented center points).

Table 1. Cutting parameters.

Factor	Lower level	Central point	Upper level
Cutting speed, v_c (m/min)	60	90	120
Feed, f (mm/rev)	0.10	0.25	0.40
Depth of cut, a_p (mm)	0.20	0.35	0.50

Figure 1(a) presents the component in its final form and dimensions and Fig. 1(b) shows a specimen under metrological assessment. A TESA Micro-Hite 3D coordinate measurement machine (CMM) was used to measure the following deviations: diameter and circularity of $\text{Ø}48$ mm, concentricity between $\text{Ø}48$ mm and $\text{Ø}58$ mm and parallelism between the shoulders associated with $\text{Ø}58$ mm. Surface roughness was assessed with a Taylor-Hobson Surtronic 25 roughness meter set to a cut-off of 0.8 mm. These data were used in the analysis of variance (ANOVA) in order to investigate the influence of each input and their interactions employing a significance level of 5%.



(a) Designed component.

(b) Specimen under assessment

Fig. 1. (a) Component final dimensions and (b) specimen under assessment in CMM.

Finally, samples were cut from selected specimens for microstructure and microhardness assessment using an abrasive water jet machine (Flow model 3M WMC with 74 kW power) in order to avoid any thermal damage. The samples were ground, polished and etched in a solution of 2% Nital in ethanol. Microstructure analysis was performed using a Zeiss Axio Observer.D1m optical microscope and subsurface microhardness distribution was evaluated with a Shimadzu HMV-2T hardness tester applying a load of 50 gf during 20 seconds.

3. Results and Discussion

The results concerned with surface alterations (dimensional and geometric deviations) induced by hard turning of AISI 52100 steel are given in Figs. 2 to 10. With regard to the diameter deviation ($\text{Ø}48$ mm), the Pareto chart presented in Fig. 2 shows that feed, f , the interaction between feed and depth of cut, a_p , and depth of cut are, in this order, the factors and interaction which significantly affect diameter deviation. The interaction plot shown in Fig. 3 indicate that for a feed of $f = 0.10$ mm/rev, the elevation of depth of cut has a negligible influence on diameter deviation, however, $f = 0.40$ mm/rev not only promoted higher deviation but also triggered the undesirable influence of depth of cut.

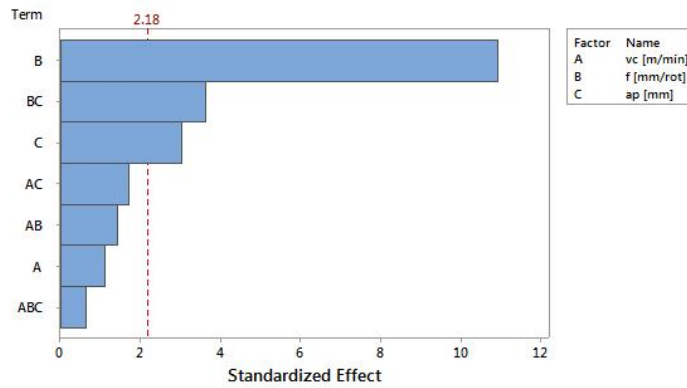


Fig. 2. Pareto chart for diameter deviation.

According to Kalyan Kumar and Choudhury [9], this behavior can be explained by the fact that an increase in feed and/or depth of cut elevates the shear area and require higher cutting forces, thus increasing dimensional error. Moreover, larger elastic deformation of the workpiece is observed, reducing the effective depth of cut and affecting the final dimensions. On its hand, when lower depths of cut are employed, lower cutting forces and elastic deformation of the part are obtained, thus leading to an increase in the effective depth of cut, i.e., the actual depth of cut becomes closer to the planned value. This process continues in a regenerative cycle causing the elevation of the circularity error. The fact that the diameter deviation was higher when $a_p = 0.20$ mm in comparison with $a_p = 0.50$ mm may be explained by the fact that plowing was dominant over shearing due to the difficulty of the cutting edge to penetrate the work material (caused by the presence of tool chamfer in the former associated with the high hardness of the latter).

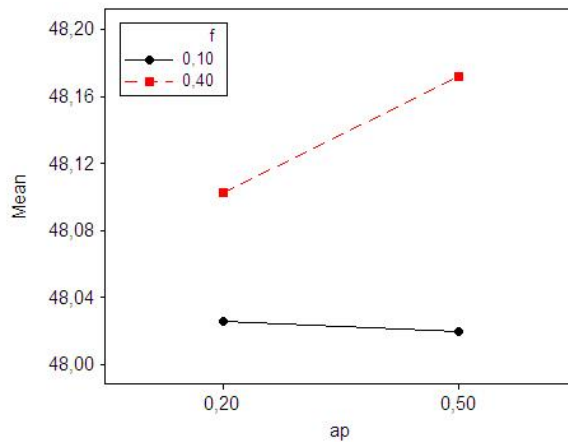


Fig. 3. Interaction effects plot for diameter deviation.

Figures 4 and 5 show, respectively, the Pareto chart and main effects plot for the circularity deviation. In this case, feed is the only significant factor and the greater its value, the larger the circularity error. The higher the feed, the higher the cutting forces and elastic deformation of the workpiece and, consequently, the circularity error.

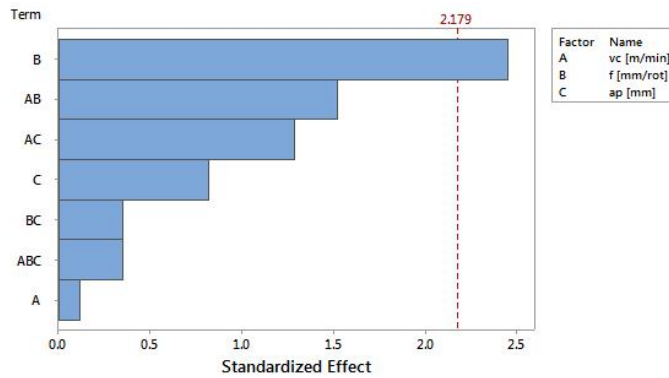


Fig. 4. Pareto chart for circularity deviation.

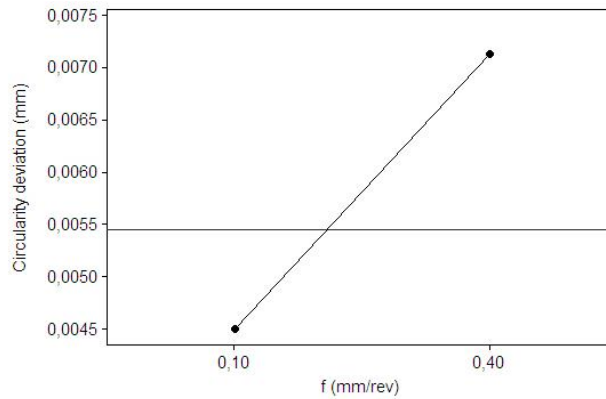


Fig. 5. Main effect plot for circularity deviation.

As far as the concentricity error is concerned, Fig. 6 shows that the influential factors encompass cutting speed, feed as well the interaction between feed and depth of cut and the third order interaction ($v_c \times f \times a_p$). Interestingly, as shown in Fig. 7, cutting speed and feed affect concentricity in opposite ways while concentricity increases drastically with the former parameter, it is reduced as feed is elevated. This behavior can be explained by the relationship between these factors and heat generation and its transfer, i.e., the elevation of cutting speed results in more energy being converted into heat in the cutting zone and in an increase in the amount of heat conducted to the workpiece, which causes its thermal expansion and leads to higher concentricity error, since the two diameters ($\varnothing 48$ mm and $\varnothing 58$ mm) are generated at different stages of the operation. Although the elevation of feed also results in more heat generation, the shear area is elevated, allowing larger amounts of heat to be conducted away from the workpiece by thicker chips (while chip thickness is reduced when cutting speed is increased). Furthermore, the elevation of cutting speed requires higher rotational speed from the lathe main spindle, which may lead to vibration of the workpiece and impair circularity deviation.

Comparing Figs. 5 and 7, it can be noted that feed affects circularity and concentricity deviations in reverse ways. The elevation of feed results in higher

forces, especially in the feed direction, consequently, higher circularity deviation is expected when feed is increased, as can be seen in Fig. 5. The reason why the elevation of feed reduces the concentricity deviation (Fig. 7) may be associated with the fact that concentricity is a related feature assessed between two distinct diameters of Ø48 mm and Ø58 mm (while circularity is an individual feature reporting how close the selected surface is from a true circle). Since both diameters were turned at the same feed value, the decrease in concentricity observed as feed is elevated may be attributed to lesser friction of the tool against the workpiece and shorter time required for the tool to complete its path. Consequently, the undesirable influence of heat and thermal expansion is minimized at the highest feed value.

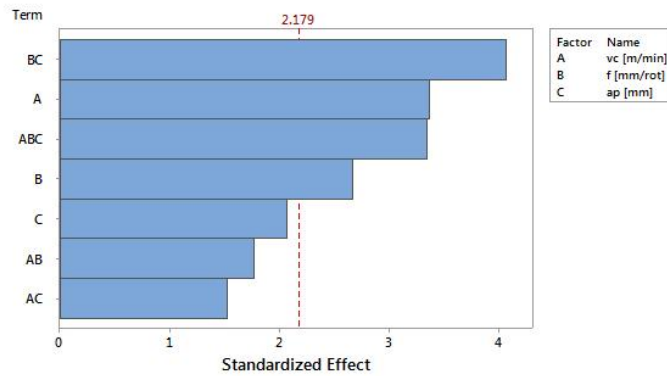


Fig. 6. Pareto chart for concentricity deviation.

As far as the interactions $f \times a_p$ and $v_c \times f \times a_p$ are concerned, Fig. 8 suggests that for $f = 0.10$ mm/rev, increasing depth of cut results in a drastic reduction in concentricity, whereas this deviation increases slightly with depth of cut for $f = 0.50$ mm/rev. Considering that the turning force components are directly related to these parameters, it is plausible that a decrease in concentricity observed when depth of cut is elevated and feed kept in 0.10 mm/rev is due to elastic deformation, as proposed by Kalyan Kumar and Choudhury [9] and discussed above.

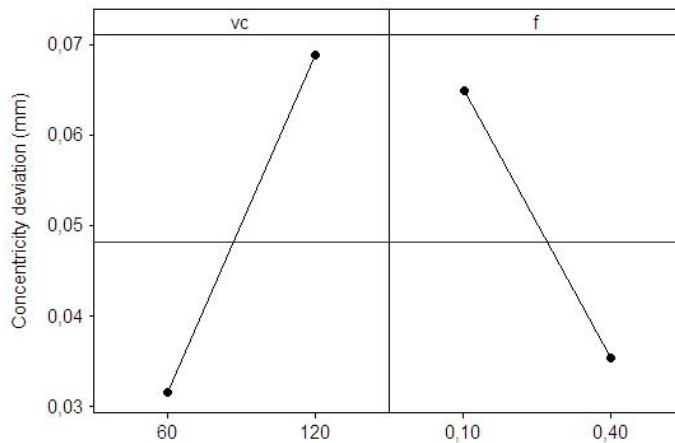


Fig. 7. Main effects plots for concentricity deviation.

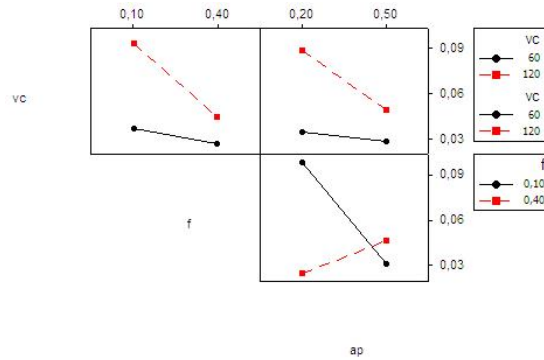


Fig. 8. Interaction plots for concentricity deviation.

Figures 9 and 10 present the results of the analysis of variance for parallelism deviation. In this case, depth of cut is the only significant factor and its elevation causes an increase in the parallelism error. The reason for that resides in the elevation of the torque resulting from the product of passive force and workpiece overhang (lever arm). As depth of cut increases, the passive force is elevated, as well as the torque. Furthermore, since the shoulders are 20 mm apart, there will be an appreciable increase in the moment applied to the shoulder, which is farther from the machine tool chuck.

Although the Pareto chart shown in Fig. 9 indicates that the influence of feed cannot be considered statistically significant for a confidence level of 95%, Fig. 10 indicates that its influence is similar to that of depth of cut, i.e., its elevation increases cutting forces and impairs parallelism, even though its influence predominantly affects feed force.

The Pareto chart of Fig. 11 depicts the influence of cutting parameters on machined surface roughness (*Ra* parameter) and Fig. 12 shows the relationship between feed and surface roughness. It can be noted that feed is the only significant factor and the reason for that resides in the fact that feed and tool nose radius are the only factors involved in the theoretical determination of surface roughness. Since the influence of the latter was not investigated in the present work, feed would be expected to be the most relevant parameter. Considering that the cutting inserts used in this work possess a nose radius of 0.8 mm, the theoretical roughness values for feeds of 0.1 mm/rev and 0.4 mm/rev are, respectively, $Ra = 0.4 \mu\text{m}$ and $Ra = 6.41 \mu\text{m}$. Figure 12 shows that the experimental values are near to the theoretical ones, moreover, $Ra = 0.4 \mu\text{m}$ matches those obtained by grinding.

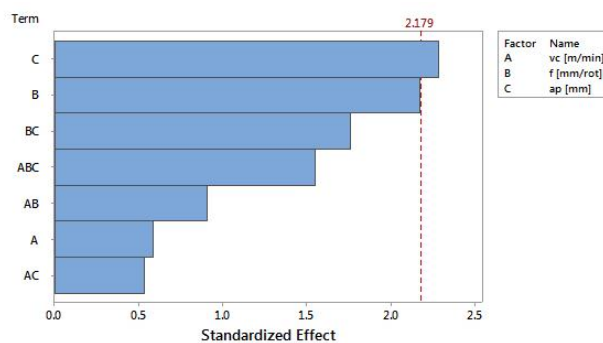


Fig. 9. Pareto chart for parallelism deviation.

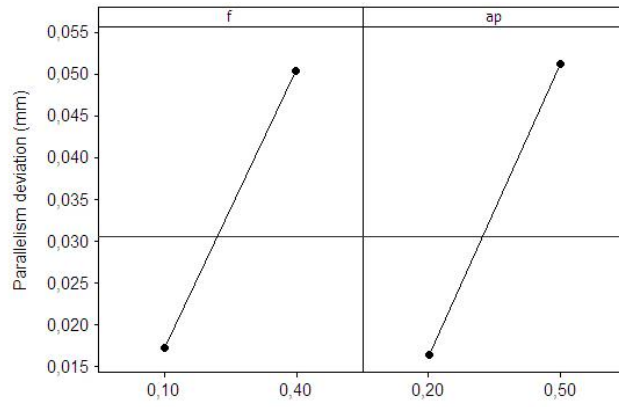


Fig. 10. Main effects plot for parallelism deviation.

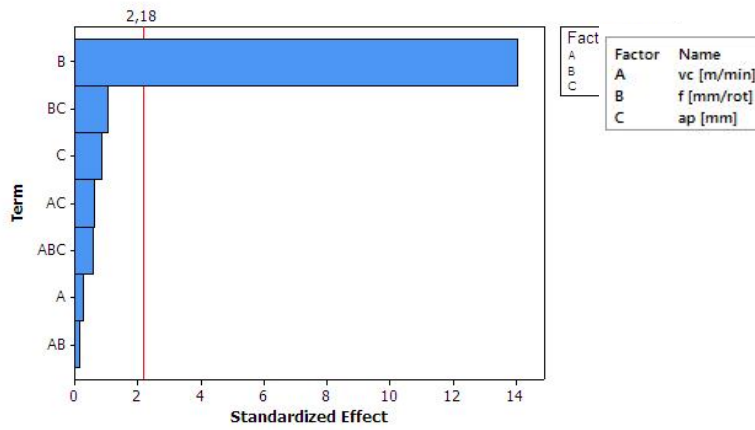


Fig. 11. Pareto chart for surface roughness.

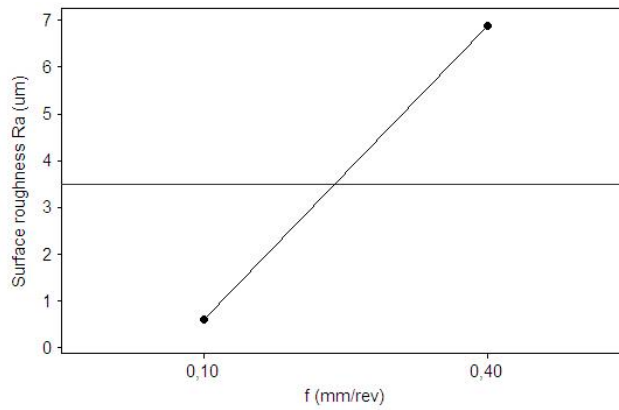


Fig. 12. Main effect plot for surface roughness.

Figure 13 presents the subsurface alterations induced by hard turning of AISI 52100 steel under selected cutting conditions, assessed in terms of microhardness distribution beneath the surface and microstructure changes. The cutting conditions were chosen in a fashion which allows the determination of the influence of one factor at a time, therefore, micrograph **A** and microhardness curve **A** represent the mildest cutting condition ($v_c = 60$ m/min, $f = 0.1$ mm/rev and $a_p = 0.2$ mm), where substantial changes in microhardness and in the martensitic microstructure are not evident. The microhardness recorded on the surface was 689 HV_{0.05} and its maximum value reached 712 HV_{0.05} at a depth of 29 μ m beneath the surface). Furthermore, curve **A** presented the lowest scatter in the data.

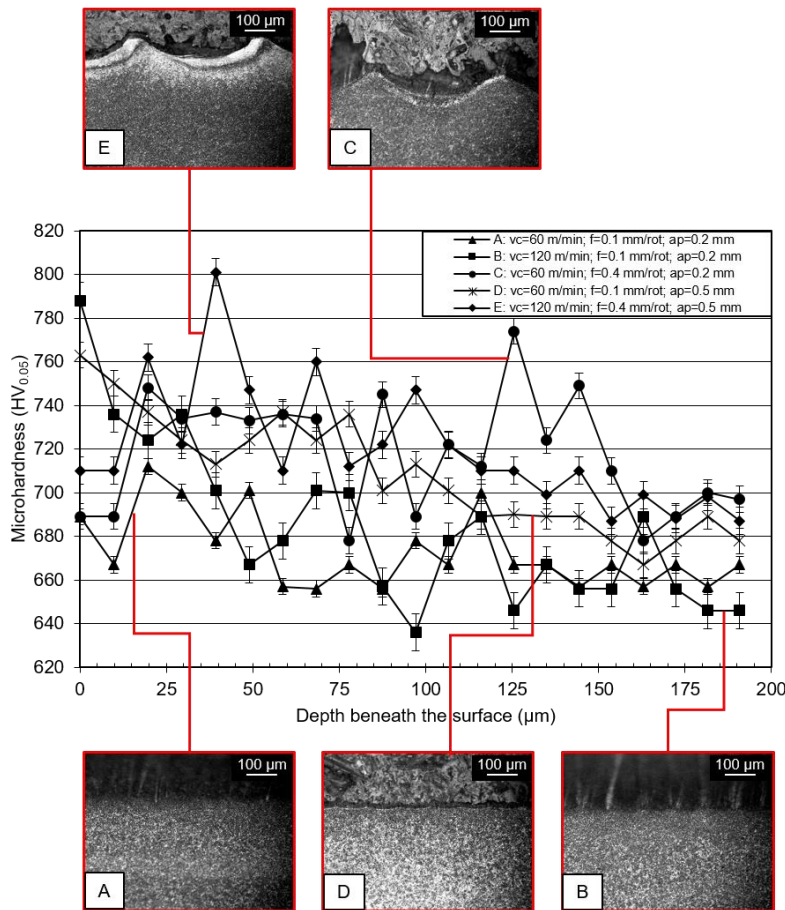


Fig. 13. AISI 52100 steel microstructure and microhardness distribution beneath the surface for selected cutting conditions.

When cutting speed is increased to $v_c = 60$ m/min while feed and depth of cut are kept at their lower levels ($f = 0.1$ mm/rev and $a_p = 0.2$ mm, respectively), microhardness values increase dramatically near the surface (788 HV_{0.05}), followed by a sudden decrease, as shown in curve **B**, nevertheless, the magnification employed to produce the images does not allow identifying changes in microstructure (micrograph **B**). Curve **C** and micrograph **C** represent the cutting condition $v_c = 60$ m/min, $f = 0.4$ mm/rev and $a_p = 0.2$ mm, therefore, comparing these data with those

from micrograph and microhardness curve **A**, one can assess the influence of feed. Additionally to the large feed marks and the tool nose radius imprinted on the work material surface, a shallow and faint white layer can be noted, thus suggesting the presence of a white layer. However, the microhardness value on the surface (691 HV_{0.05}) does not corroborate this conjecture, which is unlikely since cutting temperature is probably low ($v_c = 60$ m/min) and the large chip thickness allows efficient conduction of heat away from the workpiece. The influence of depth of cut on microhardness distribution and subsurface alterations can be appraised by comparing micrograph **D** and microhardness curve **D** ($v_c = 60$ m/min, $f = 0.1$ mm/rev and $a_p = 0.5$ mm) with micrograph **A** and microhardness curve **A** ($v_c = 60$ m/min, $f = 0.1$ mm/rev and $a_p = 0.2$ mm), respectively. Despite the appreciable increase in the microhardness value on the surface (763 HV_{0.05}), micrograph **A** does not present evidence of a white layer and a possible reason for hardness elevation may be work hardening. Finally, micrograph **E** and microhardness curve **E** were produced after turning AISI 52100 steel employing cutting conditions in their upper level ($v_c = 120$ m/min, $f = 0.4$ mm/rev and $a_p = 0.5$ mm). In addition to feed and tool nose marks, evidence of a white layer can be noted near the surface, however, heat conduction from the cutting zone was boosted by the large feed and depth of cut values used.

4. Conclusions

After conducting continuous dry finish turning tests on hardened AISI 52100 (60 ±2 HRC) using titanium carbide reinforced alumina tools and assessing surface (dimensional and geometric deviations) and subsurface alterations (microstructure and microhardness alterations), the following conclusions can be drawn:

- Diameter error increased mainly with the elevation of feed, followed by depth of cut. This behavior is associated with the elevation of cutting forces as the shear area is elevated.
- Feed is the only cutting parameter that significantly affects the circularity deviation, for the same reason previously mentioned.
- Concentricity deviation is affected by cutting speed, feed and by the interactions between feed and depth of cut and the third order interaction. While an increase in heat generation and conduction to the workpiece is responsible for larger concentricity values when cutting speed is elevated, the higher the feed, the lower the concentricity error owing to the increase in the shear area, throughout which heat is conducted away from the cutting zone.
- Depth of cut is the only significant factor affecting parallelism deviation due to the increase in the torque caused by higher passive force values observed when turning under elevated depths of cut.
- Feed was the only cutting parameter that statistically affected surface roughness and *Ra* values equivalent to grinding were obtained.
- Higher surface microhardness values were obtained when combining higher cutting speed and lower feed and depth of cut. Increasing cutting speed with feed and depth of cut results in higher amounts of heat together with a shear plane area sufficiently high to allow heat conduction away from the workpiece.
- Under the cutting conditions employed in this work, evidence of microstructure alterations was observed under the most severe cutting condition only.

Nomenclatures

a_p	Depth of cut, mm
f	Feed, mm/rev
v_c	Cutting speed, m/min
Ra	Theoretical roughness, μm

Abbreviations

ANOVA	Analysis of Variance
CMM	Coordinate Measuring Machine
PcBN	Polycrystalline Cubic Boron Nitride

Acknowledgements

Authors would like to thank the following research agencies in Brazil for supporting this research project: CNPq, CAPES and FAPEMIG.

References

1. Bartarya, G.; and Choudhury, S.K. (2012). State of the art in hard turning. *International Journal of Machine Tools and Manufacture*, 53(1), 1-14.
2. Qian, Li; and Hossan, M.R. (2007). Effect on cutting force in turning hardened tool steels with cubic boron nitride inserts. *Journal of Materials Processing Technology*, 191(1-3), 274-278.
3. Zhou, J.M.; Andersson, M.; and Stahl, J.E. (2004). Identification of cutting errors in precision hard turning process. *Journal of Materials Processing Technology*, 153-154, 746-750.
4. Hosseini, S.B.; Beno, T.; Klement, U.; Kaminski, J.; and Rytberg, K. (2014). Cutting temperatures during hard turning - Measurements and effects on white layer formation in AISI 52100. *Journal of Materials Processing Technology*, 214(6), 1293-1300.
5. Tönshoff, H.K.; Arendt, C.; and Amor, R.B. (2000). Cutting of hardened steel. *CIRP Annals - Manufacturing Technology*, 49(2), 547-566.
6. Guo, Y.B.; Warren, A.W.; and Hashimoto, F. (2010). The basic relationships between residual stress, white layer, and fatigue life of hard turned and ground surfaces in rolling contact. *CIRP Journal of Manufacturing Science and Technology*, 2(2), 129-134.
7. Bernardos, P.G.; Mosailos, S.; and Vosniakos, G.C. (2006). Prediction of workpiece elastic deflections under cutting forces in turning. *Robotics And Computer-integrated Manufacturing*, 22(5-6), 505-514.
8. Fan, K.-C.; Chen, H.-M.; and Kuo, T.-H.. Prediction of machining accuracy degradation of machine tools. *Precision Engineering*, 36(2), 288-298.
9. Kalyan Kumar, K.V.B.S.; and Choudhury, S.K. (2008) Investigation of tool wear and cutting force in cryogenic machining using design of experiments. *Journal of Materials Processing Technology*, 203(1-3) 95-101.
10. Henzold, G.; (2006). *Geometrical dimensioning and tolerancing for design, manufacturing and inspection: a handbook for geometrical product specification using ISO and ASME standards*, Oxford: Elsevier.

11. Weck, M.; McKeown, P.; Bonse, R.; and Herbst, U. (1995) Reduction and compensation of thermal errors in machine tools. *CIRP Annals*, 44(2), 589-598.
12. Ueda, T.; Al Huda, M.; Yamada, K.; Nakayama, K.; and Kudo, K. (1999). Temperature measurement of CBN tool in turning of high hardness steel. *CIRP Annals - Manufacturing Technology*, 48(1), 63-66.
13. Müller, B.; Renz, U.; Hoppe, S.; and Klocke, F. (2004) Radiation thermometry at a high-speed turning process. *Journal of Manufacturing Science and Engineering*, 126(3), 488-496.
14. Han, S.; Melkote, S.N.; Haluska, M.S.; and Watkins, T.R. (2008). White layer formation due to phase transformation in orthogonal machining of AISI 1045 annealed steel. *Materials Science and Engineering: A*, 488(1-2), 195-204.
15. Umbrello, D.; and Filice, L. (2009). Improving surface integrity in orthogonal machining of hardened AISI 52100 steel by modeling white and dark layers formation. *CIRP Annals*, 58(1), 73-76.
16. Biček, M.; Dumont, F.; Courbon, C.; Pusavec, F.; Rech, J.; and Kopac, J. (2012). Cryogenic machining as an alternative turning process of normalized and hardened AISI 52100 bearing steel. *Journal of Materials Processing Technology*, 212(12), 2609-2618.
17. Sandvik Coromant (2017). Turning tools, p. A264. Retrieved March 16, 2018, from http://sandvik.ecbook.se/se/en/turning_tools_2017/.
18. Montgomery, D.C. (1997). *Design and analysis of experiments* (5th ed.). New York: John Wiley & Sons, Inc.